

Photon + Hadron Production in High Energy Deuteron (Proton)-Nucleus Collisions

Jamal Jalilian-Marian

Institute for Nuclear Theory, University of Washington, Seattle, WA 98195

Abstract

We apply the Color Glass Condensate formalism to photon + hadron production cross section in high energy deuteron (proton)-gold collisions at RHIC. We investigate the dependence of the production cross section on the angle between the produced hadron and photon for various rapidities and transverse momenta. It is shown that the angular correlation between the produced hadron and photon is a sensitive probe of the saturation dynamics.

1 Introduction

The recent RHIC results on the suppression of the hadron transverse momentum spectra in deuteron-gold collisions, as compared to proton-proton collisions, in the forward rapidity region [1] have caused a major excitement in the RHIC community. While the observed suppression was qualitatively predicted by the Color Glass Condensate (CGC)¹ based approaches [3], and verified by more quantitative analysis [4, 5], there have been newer models introduced recently which can also fit the data [6]. Measurement of different processes, for example prompt photon [7] or heavy quark pair production [8], at RHIC can therefore help establish the dominance of the saturation dynamics in the forward rapidity region at RHIC.

Unlike hadron production, electromagnetic processes such as prompt photon or dilepton [9] production do not involve hadronization of the final state and are therefore a cleaner process in which to investigate the saturation dynamics. Due to smallness of the electromagnetic coupling constant, however, these processes are rare and require high beam luminosity and/or long running times of the machine. Nevertheless, in order to clarify the underlying physics of particle production in forward rapidity region at RHIC and eventually in mid or forward rapidity LHC, it is essential to measure photons, dileptons, etc. at RHIC. A measurement of photon production in the forward rapidity region, for example, can distinguish between recombination models and the Color Glass Condensate physics since one does not expect recombination effects to be relevant for prompt photon production while one expects a suppression pattern for prompt photons very similar to hadrons in deuteron (proton)-nucleus collisions in the Color Glass Condensate formalism.

Two particle correlations are known to be a sensitive probe of saturation dynamics. While the two hadron correlation function in mid rapidity is expected to broaden due to multiple scattering, it is expected to disappear as one measures two widely separated (in rapidity) hadrons due to the small x quantum evolution [10]. This qualitative expectation is verified by preliminary data from RHIC [11]. A more quantitative theoretical analysis of the two hadron correlation in the Color Glass Condensate formalism [12] is however quite challenging due to presence of 3 and 4-point functions of Wilson lines and therefore requires making approximations (for example, large N_c or Gaussian ansatz) and assumptions which may affect the outcome of the analysis. Furthermore, since the measured hadrons are at low to intermediate transverse momenta, non-perturbative effects may play an important role.

Therefore, in this brief note, we consider production of a hadron and a photon as the cleaner and theoretically simpler process in which to investigate angular correlations and the role of saturation physics. This process has the further advantage that it is not expected to suffer from possible recombination effects and can therefore help establish/constrain validity of applying the Color Glass Condensate formalism to deuteron-nucleus collisions at RHIC. Experimentally, it is possible to measure this process at RHIC, using the STAR detector, for example, even though one will most likely need another deuteron-gold run for improved statistics and detector coverage.

¹See [2] for reviews and extensive references.

As shown in [5], one probes the very large x region in the deuteron wave function and the very small x region in the target wave function (see Fig. 10 in [5] for the values of x contributing to single hadron production). In this kinematics, one can treat the incoming deuteron (proton) as a dilute object, consisting of quarks and gluons [13] with a possible nuclear modification of the deuteron wave function which should be very small for the typical x and Q^2 involved. On the other hand, the values of x probed in the target wave function are very small, $O(10^{-3} - 10^{-4})$. Therefore, it is essential to include the high gluon density effects in the target.

The quark-photon production cross section in quark-nucleus scattering has been calculated in the Color Glass Condensate formalism in [9]. We use this cross section and convolute it with quark (anti-quark) distributions in a deuteron (proton) and quark-hadron fragmentation function to make predictions for hadron-photon angular correlations at RHIC and LHC. To probe the smallest x possible in a given process in a hadron-hadron (nucleus-nucleus) collider environment, one needs to be in the forward rapidity region. RHIC has the further advantage of having a very unique forward rapidity capability, with plans for detector upgrades. One therefore can expect to be able to measure the hadron-photon correlation in a wide kinematic region at RHIC. For example, the STAR collaboration will be able to measure hadrons and photons at rapidities $y = 0$ and 4 and study their correlations.

2 The Scattering Cross Section

The scattering cross section for production of a massless on-shell quark with momentum \vec{l} and a real photon with momentum \vec{k} was derived in [9]. It is given by

$$\begin{aligned} \frac{d\sigma^{q(p) A \rightarrow q(l) \gamma(k) X}}{d^2b_t dk_t^2 dl_t^2 dy_\gamma dy_l d\theta} &= \frac{e_q^2 \alpha_{em}}{\sqrt{2}(2\pi)^2} \frac{k^-}{k_t^2 \sqrt{s}} \frac{1 + (\frac{l^-}{p^-})^2}{[k^- \vec{l}_t - l^- \vec{k}_t]^2} \\ &\delta\left[x - \frac{l_t}{\sqrt{s}} e^{y_l} - \frac{k_t}{\sqrt{s}} e^{y_\gamma}\right] \left[2l^- k^- l_t k_t \cos\theta + k^-(p^- - k^-) l_t^2 + l^-(p^- - l^-) k_t^2\right] \\ &\int dr_t r_t J_0[r_t |\vec{l}_t + \vec{k}_t|] N(b_t, r_t, x_g) \end{aligned} \quad (1)$$

where the incoming quark has momentum p , the photon and outgoing quark rapidities are defined via $k^- = \frac{k_t}{\sqrt{2}} e^{y_\gamma}$ and $l^- = \frac{l_t}{\sqrt{2}} e^{y_l}$. The angle θ is the opening angle between the final state quark and photon defined as $\cos\theta \equiv \frac{l_t \cdot k_t}{l_t k_t}$, with respect to the produced quark axis. The dipole cross section N satisfies the JIMWLK equation and has all the multiple scattering and small x evolution effects encoded. It is defined as

$$N(b_t, r_t, x_g) = \frac{1}{N_c} Tr \langle 1 - V^\dagger(x_t) V(y_t) \rangle \quad (2)$$

with $b_t \equiv (x_t + y_t)/2$ and $r_t \equiv x_t - y_t$. The dipole cross section depends on Bjorken x_g via the JIMWLK renormalization group equations. In the present case, it is related to the

photon and final state quark rapidities and transverse momenta via

$$x_g = \frac{1}{\sqrt{s}} [k_t e^{-y_\gamma} + l_t e^{-y_l}]. \quad (3)$$

In order to compute the hadron + photon production cross section, we would need to convolute the above partonic cross section with the quark and anti-quark distributions of a deuteron (proton) and quark-hadron fragmentation function. However, before doing that, it is instructive to investigate in some detail, the properties of the above cross section. Specifically, we would like to investigate the dependence of this cross section on the angle between the produced quark and photon. In order to do this, we isolate the parts of the cross section which depend on the angle and ignore the rest of the kinematic factors for the moment. Therefore we define the angle dependent part of the cross section as

$$I(\theta) \equiv \frac{[2l^- k^- l_t k_t \cos \theta + k^-(p^- - k^-) l_t^2 + l^-(p^- - l^-) k_t^2]}{[k^- \vec{l}_t - l^- \vec{k}_t]^2} \int dr_t r_t J_0[r_t |\vec{l}_t + \vec{k}_t|] N(b_t, r_t, x_g) \quad (4)$$

Without making any assumptions about the specific form of the dipole cross section N , it is clear from the factor $\frac{1}{[k^- \vec{l}_t - l^- \vec{k}_t]^2}$ that $I(\theta)$ diverges when the momenta of produced quark and photon are parallel ($\theta \rightarrow 0$). This is the standard collinear divergence present in perturbation theory and is not affected by saturation physics. On the other hand, when $\vec{l}_t = -\vec{k}_t$, then $|\vec{l}_t + \vec{k}_t| \rightarrow 0$ and the integral over the dipole size r_t is divergent. This is taken care of by demanding color neutrality of the target which would cut the dipole size off at $r_t \sim 1 fm$. It should be noted that this is different from the single hadron production case where, at finite transverse momentum of the produced hadron, the integral over dipole size r_t is always finite.

To proceed further, we need to know the dipole profile $N(b_t, r_t, x_g)$. It satisfies the JIMWLK equation and therefore can be obtained by solving the JIMWLK equation with a suitable boundary condition. However, this is highly nontrivial and in practice, it is much more convenient to use one of the available parameterizations such as the KKT profile [4]. In this model, the dipole profile is given by

$$N(b_t, r_t, x_g) = \left(\exp \left[-\frac{1}{4} [r_t^2 Q_s^2(y)]^{\gamma(y, r_t)} \right] - 1 \right) \quad (5)$$

where the anomalous dimension $\gamma(y, r_t)$ is

$$\gamma(y, r_t) = \frac{1}{2} \left(1 + \frac{\xi(y, r_t)}{\xi(y, r_t) + \sqrt{2\xi(y, r_t) + 28\zeta(3)}} \right) \quad (6)$$

and

$$\xi(y, r_t) = \frac{\log 1/r_t^2 Q_0^2}{(\lambda/2)(y - y_0)}. \quad (7)$$

The saturation scale is given by $Q_s(y) = Q_0 \exp[\lambda(y - y_0)/2]$ with $y = \ln 1/x_g$ and $y_0 = 0.6$, $\lambda = 0.3$. This is the form of the dipole profile we will use for our numerical analysis.

However, it is instructive to consider the analytic behavior of $I(\theta)$. This is possible in two limits; when $\gamma(y, r_t)$ is either $1/2$ or 1 . The former corresponds to the BFKL and saturation region while the later is the case when one has the standard DGLAP anomalous dimension. It turns out that the case $\gamma = 1/2$ is very close to the actual value of the anomalous dimension when one does the integral numerically. Therefore, we use this value in our analytic estimates. The integral over the dipole size r_t can be then done exactly and gives

$$\int dr_t r_t J_0[r_t |\vec{l}_t + \vec{k}_t|] N(b_t, r_t, x_g)|_{\gamma=1/2} = \frac{16}{Q_s^2 [1 + \frac{16|\vec{l}_t + \vec{k}_t|^2}{Q_s^2}]^{\frac{3}{2}}} \quad (8)$$

Strictly speaking, the integral over r_t is divergent when $\theta = \pi$ if $|l_t| = |k_t|$ and needs to be regularized by confinement scale $r_t \sim 1fm$. To avoid the numerical complications of regularization, in this work we stay away from $\theta = \pi$ point and keep in mind that the expression in (8) is not valid² at $\theta = \pi$. Using this expression in $I(\theta)$ gives

$$I(\theta) \rightarrow \frac{k_t e^{-y_l + y_\gamma} [\vec{l}_t + \vec{k}_t]^2}{l_t [(\frac{k_t^-}{l_t^-}) \vec{l}_t - \vec{k}_t]^2} \frac{1}{Q_s^2} \frac{1}{[1 + \frac{16|\vec{l}_t + \vec{k}_t|^2}{Q_s^2}]^{\frac{3}{2}}} \quad (9)$$

This form of $I(\theta)$ shows the angular dependence of the cross section most clearly and can serve as a guide understanding the exact numerical results shown later. Note that the above expression does not depend on whether k_t is larger or smaller than the saturation scale Q_s and is therefore valid in both the saturation and BFKL regions to the extent that $\gamma \simeq 1/2$ remains a good approximation.

In Fig. (1) we show the function $I(\theta)$ where both the produced photon and quark are in mid rapidity (RHIC) and for the case where both have equal transverse momenta. The solid line is when both quark and photon have transverse momenta $l_t = k_t = 1GeV$ and the dashed line is when both transverse momenta are $3GeV$. For ease of comparison, we normalize the two curves at the smallest angle. At the smaller momentum $1GeV$, the "away" side ($\theta \rightarrow 0$) correlation is flat while for higher momentum $3GeV$, the away side peak is returning. This is mainly due to the increase of x_g , as given by (3) and therefore a decrease of $Q_s^2(x_g)$ which indicates a weakening of the gluon saturation effects in the target nucleus. It should be noted that introduction of an "isolation" procedure experimentally in the photon measurement would cutoff the collinear divergence present in $I(\theta)$ which is apparent in the small angle limit in Fig. (1). Since the isolation cuts needed will depend on the detector geometry after a possible upgrade and are not known at the moment, we do not consider an isolation cut on the photon.

In Fig. (2) we show the angular correlation function $I(\theta)$ at different rapidities. The solid line shows the case when both particles are in mid rapidity while the dashed line is

²Also, due to the choice of $\gamma = 1$, the high transverse momentum limit of the dipole cross section is not reproduced correctly, but this is of minor importance for $\theta \rightarrow \pi$ since in this limit the magnitude of the argument of the dipole cross section, $|\vec{l}_t + \vec{k}_t| \rightarrow 0$, is always less than the saturation scale. We emphasize that in the numerical analysis, the exact form of γ is kept so that the high transverse momentum limit of the dipole cross section is correctly reproduced.

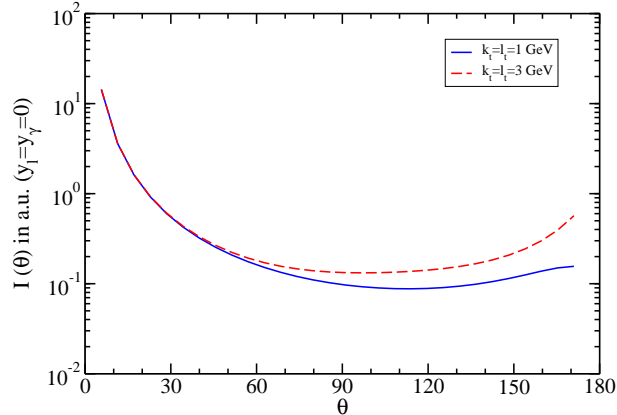


Figure 1: The angular part of the cross section, $I(\theta)$ in mid rapidity RHIC.

when the produced quark is at $y = 4$ while the produced photon is in mid rapidity. In both cases, the transverse momenta of both particles is 3GeV . This time, however, the two curves are normalized at the highest angle. As before, the angular correlation function diverges in mid rapidity when $\theta \rightarrow 0$ due to the unregularized collinear divergence. we

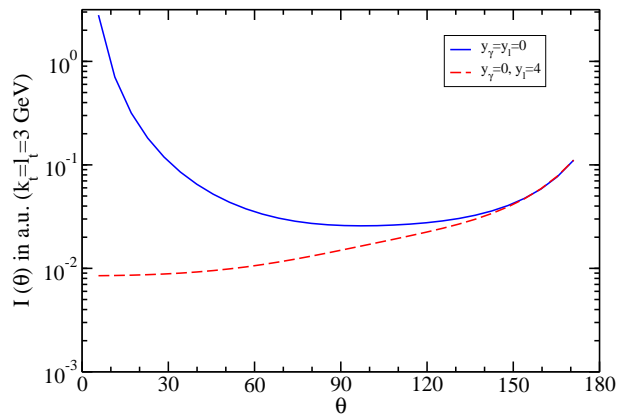


Figure 2: Rapidity dependence of $I(\theta)$ at different transverse momenta.

note that there is no collinear divergence ($\theta \rightarrow 0$) in the case when the rapidity separation is so large, $\Delta y = 4$, and when $l_t = k_t = 3\text{GeV}$ while the mid rapidity correlation function is collinear divergent.

Finally, we consider the case when both produced partons are in the forward rapidity region, $y_l = y_\gamma = 4$. In this kinematics, one is restricted to small momenta due to the available phase space so we consider $l_t = k_t = 1\text{GeV}$ as well as $l_t = k_t = 1.7\text{GeV}$ which is very close to the upper limit allowed by kinematics. Note that the two curves are not normalized like the previous figures. Again in the small angle limit, one is probing the collinear divergence present in the angular function which shows up as sharp rise of $I(\theta)$.

In a realistic experimental set up, this will be tamed by the isolation cut imposed on the photon.

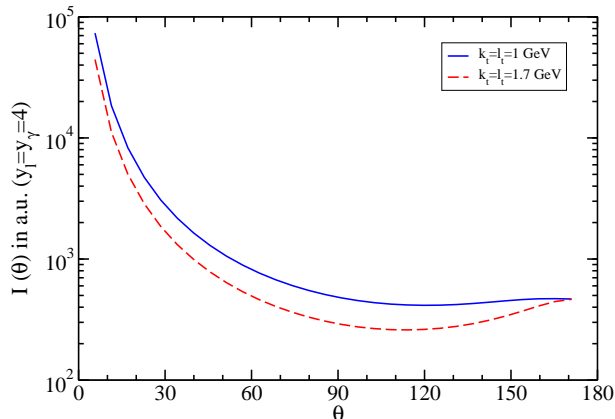


Figure 3: The angular correlation $I(\theta)$ in the forward rapidity region $y_l = y_\gamma = 4$.

To relate our results for the parton production to the case hadron + photon production, we need to convolute the partonic cross section in (1) with the parton distribution function in a deuteron and the quark-hadron fragmentation function. The hadron +photon production cross section can then be written as

$$\frac{d\sigma^{dA \rightarrow h(q)\gamma(k)X}}{d^2b_t dk_t^2 dq_t^2 dy_\gamma dy_h d\theta} = \int_{z_{min}}^1 \frac{dz}{z^2} \int dx f_{q/d}(x, Q^2) D_{h/q}(z, Q^2) \frac{d\sigma^{q(p)A \rightarrow q(l)\gamma(k)X}}{d^2b_t dk_t^2 dl_t^2 dy_\gamma dy_l d\theta} \quad (10)$$

where a sum over different quark and anti-quark flavors is understood and y_h, q_t are the rapidity and transverse momentum of the produced hadron. We have neglected hadron masses so that the rapidity of the produced quark and hadron are the same. The momentum fraction z is defined as $z = q_t/l_t = q^-/l^-$ and its minimum value in (10) is given by $z_{min} \equiv \frac{q_t}{\sqrt{s}} \left[\frac{1}{1 - \frac{k_t}{\sqrt{s}}} \right] e^{y_h - y_\gamma}$. Since the nuclear modification (shadowing) of the deuteron wave function is expected to be small in this kinematics, it is ignored. We use the GRV98 set of parton distribution functions [14] as well the KKP hadron fragmentation functions [15]. The integral over x is simple and can be done using the delta function present in the partonic cross section so that there is effectively only one integration to perform.

In Fig. (4) we show the invariant cross section given by (10) at mid rapidity RHIC for three different transverse momenta; $q_t = kT = 1.5 GeV$, $q_t = k_t = 3 GeV$ and $q_t = k_t = 5 GeV$. The lowest transverse momentum of the hadron considered is $\sim 1.5 GeV$ since the fragmentation functions of KKP start at $Q_0 = 1.5 GeV$. Again, all the curves are normalized to match at the lowest angle for ease of comparison. As is seen, the away side correlation is much less for smaller momenta, which in this case is comparable to the saturation scale of the nucleus $Q_s \sim 1.5 GeV$. The largest considered transverse momentum, $5 GeV$, is much larger than the saturation scale and most likely, even larger

than the so called extended scaling scale. The cross section is again much larger for the collinear configuration of the hadron and photon. This will be modified by the isolation cuts imposed by the future detector setup at RHIC. However, the rise of the correlation with higher transverse momenta is clear even without any isolation cuts. Furthermore, the isolation cuts imposed on collinear photons will not affect the large angle correlation even though it will be much easier to judge whether the away side peak is as large as, or comparable to, the near side peak which is not possible to tell without an isolation cut.

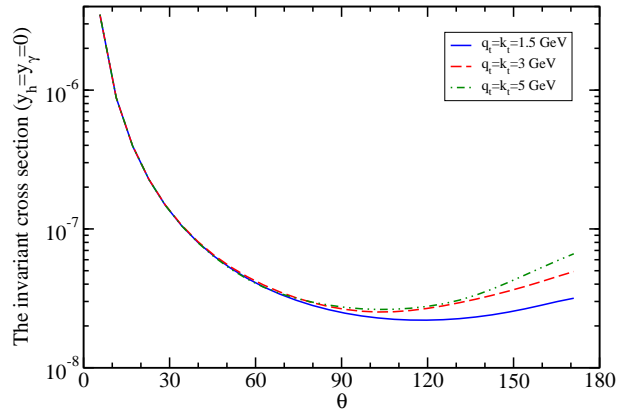


Figure 4: The invariant cross section given by (10) at different transverse momenta.

In Fig. (5) we show the invariant cross section as given by (10) at different rapidities: We consider the cases when both hadron and photon are at the same rapidity; either

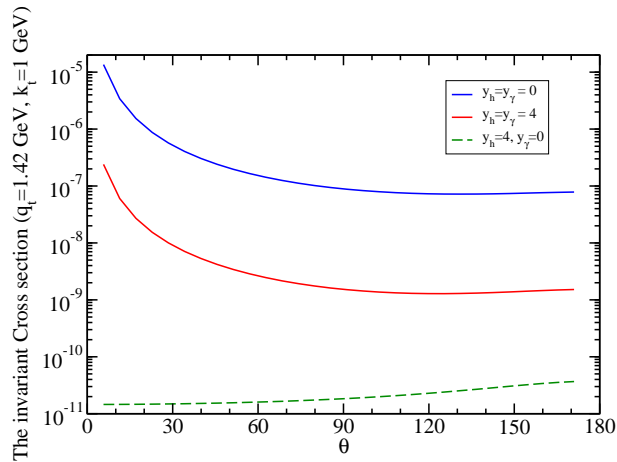


Figure 5: The invariant cross section (10) at different rapidities.

mid rapidity ($y = 0$) or forward rapidity ($y = 4$), and the case when they are far apart

in mid rapidity, i.e. when the photon is in mid rapidity and the hadron is in the forward region. We note that in the kinematics when the two particles have the same transverse momenta but are widely separated in rapidity, there is no collinear divergence due to the large factor of $e^{y_\gamma - y_h}$ in the denominator. Physically, this is easy to understand since two particles widely separated in rapidity can not be collinear for comparable transverse momenta. When the two produced particles are at the same rapidity, there is always a collinear divergence for comparable transverse momenta. We finally note that at rapidity of $y = 4$, we are very close to the edge of the kinematic limit for transverse momenta $\leq 2\text{GeV}$ which limits our ability to study the change in the away side peak with increasing transverse momenta. Having a more refined hadron or photon detection capabilities in the intermediate rapidity region will greatly help with this.

3 Discussion

We have calculated the hadron + photon production cross section in high energy deuteron-nucleus collisions at RHIC energy and investigated the dependence of the cross section on the angle between the produced hadron and photon. It is shown that the magnitude of "away" side peak depends sensitively on the transverse momenta of the particles produced and can thus be a sensitive measure of the importance of gluon saturation physics. Due to the collinear divergence present in the cross section, one needs to introduce an isolation cut for the photon. Since this is largely a matter of detector kinematics and capabilities which will improve with the possible upgrades at RHIC in the future, we do not include isolation cuts and leave this for future studies.

We used the dipole model of KKT for our quantitative studies. It is probably worthwhile to do this analysis using the other parameterizations available, once the experimental setup becomes more clear. The KKT dipole profile has been used successfully to fit the forward rapidity data without any model assumptions [5]. However, in mid rapidity RHIC, KKT dipole profile seem to require a much steeper anomalous dimension [16] or extra model assumptions [4]. Therefore, one should be cautious using the KKT parameterization in mid rapidity RHIC.

Furthermore, one can avoid the difficulties of the photon isolation cut procedure, by using hadron + dilepton production cross section in order to study the angular correlations and the role of saturation dynamics. The dilepton pair invariant mass will regulate the divergence of the photon + hadron cross section and therefore is a cleaner process to measure even though the rates are smaller. We leave this for future studies.

Finally, with the expected proton-lead run at LHC coming up in the near future, one will have a much broader rapidity coverage which will be helpful in many ways. Due to the larger center of mass energy compared to RHIC, the saturation scale will be larger at comparable rapidities so that the saturation effects will be stronger, and therefore, more robust. Furthermore, some of the proposed detectors such as CMS are expected to have very forward measurement capabilities. For example, it may be possible to study correlations at LHC between particles separated by 5-7 units of rapidity, and at the same

time, have quite a large phase space in transverse momentum available. This will greatly help our ability to study the different kinematics regions of the Color Glass Condensate by dialing the rapidity and transverse momenta of the produced particles.

Acknowledgments

The author thanks F. Gelis and W. Vogelsang for helpful discussions and F. Gelis for the use of his Fortran code for evaluating the dipole cross section. This work is supported in part by the U.S. Department of Energy under Grant No. DE-FG02-00ER41132.

References

- [1] I. Arsene *et al.* [BRAHMS Collaboration], nucl-ex/0410020; B. B. Back *et al.*, [PHOBOS Collaboration], nucl-ex/0410022; K. Adcox *et al.* [PHENIX Collaboration], nucl-ex/0410003; J. Adams [STAR Collaboration], nucl-ex/0501009.
- [2] E. Iancu and R. Venugopalan, arXiv:hep-ph/0303204; J. Jalilian-Marian and Y. V. Kovchegov, arXiv:hep-ph/0505052.
- [3] D. Kharzeev, Y. V. Kovchegov and K. Tuchin, Phys. Rev. D **68**, 094013 (2003); J. L. Albacete, N. Armesto, A. Kovner, C. A. Salgado and U. A. Wiedemann, Phys. Rev. Lett. **92**, 082001 (2004).
- [4] D. Kharzeev, Y. V. Kovchegov and K. Tuchin, Phys. Lett. B **599**, 23 (2004); J. Jalilian-Marian, Nucl. Phys. A **748**, 664 (2005).
- [5] A. Dumitru, A. Hayashigaki and J. Jalilian-Marian, arXiv:hep-ph/0506308.
- [6] R. C. Hwa, C. B. Yang and R. J. Fries, nucl-th/0410111.
- [7] R. Baier, A. H. Mueller and D. Schiff, Nucl. Phys. A **741**, 358 (2004); J. Jalilian-Marian, Nucl. Phys. A **739**, 319 (2004).
- [8] F. Gelis and R. Venugopalan, Phys. Rev. D **69**, 014019 (2004); J. P. Blaizot, F. Gelis and R. Venugopalan, Nucl. Phys. A **743**, 13 (2004), Nucl. Phys. A **743**, 57 (2004).
- [9] F. Gelis and J. Jalilian-Marian, Phys. Rev. D **66**, 014021 (2002), Phys. Rev. D **66**, 094014 (2002), Phys. Rev. D **67**, 074019 (2003).
- [10] D. Kharzeev, E. Levin and L. McLerran, Nucl. Phys. A **748**, 627 (2005) [arXiv:hep-ph/0403271].
- [11] A. Ogawa [STAR Collaboration], arXiv:nucl-ex/0408004.
- [12] J. Jalilian-Marian and Y. V. Kovchegov, Phys. Rev. D **70**, 114017 (2004).
- [13] A. Dumitru and J. Jalilian-Marian, Phys. Lett. B **547**, 15 (2002), Phys. Rev. Lett. **89**, 022301 (2002).
- [14] M. Gluck, E. Reya and A. Vogt, Eur. Phys. J. C **5**, 461 (1998) [arXiv:hep-ph/9806404].
- [15] B. A. Kniehl, G. Kramer and B. Potter, Nucl. Phys. B **582**, 514 (2000) [arXiv:hep-ph/0010289].
- [16] A. Dumitru, A. Hayashigaki and J. Jalilian-Marian, work in progress.